Load – Deflection Behavior of Rectangular R.C. Slabs with Three Edges Fixed and The Fourth Free Under Uniformly Load

● **Dr. Ali Flayeh Hassan -** Assist. Prof. ●

University of Duhok, College of Engineering, Department of Civil Engineering

Received : 07/02/2018 / Accepted : 06/05/2018
DOI Link: https://doi.org/10.17656/sjes.10069

Abstract

A method is proposed for the prediction of load – deflection relationship of rectangular R.C slabs with three edges fixed and the fourth free under uniformly distributed loading. The analysis is carried out in three stages. The first stage represents the initial pre-cracking elastic stage. In this stage, use is made of the classical plate theory to predict the load and deflection up to the cracking load. The second stage represents the elasto-plastic stage and starts from the cracking load to Johansen's yield line theory load. In this stage, the cracking of concrete and yielding of steel reinforcement are accounted for by suitability modifying the flexural rigidity. Changes that occur in the support conditions along the fixed edges due to the formation of the yield line lines at Johansen's load are also considered. In the third stage of analysis, a method based on the flow theory of rigid plastic bodies, is developed for assessing the ultimate strength as well as determining the post yield behavior of such slabs. The method takes into account the significant effect of membrane forces which are usually induced in the plane of the slab along sagging and hogging yield lines as the slab deflects. Considering equilibrium and compatibility of the deformed slab elements, load-deflection relation is derived starting from the initial compressive membrane action up to the full-depth cracking at large deflections. The rigid-perfectly plastic behavior is adopted with modification to obtain the actual maximum ultimate load including membrane action and the deflection at this ultimate load. The predicted load- deflection relationship is fairly comparable with typical load- deflection curves of restrained slabs.

Keywords Compressive membrane action; plastic theory; ultimate strength; yield lines.

Notation

A_s	Area of tensile reinforcement per unit width of slab
a	Depth of the equivalent rectangular compression block of concrete
C	Compressive force on concrete per unit width of slab
d	Effective depth of slab
e	Plastic axial elongation at mid – depth of slab
f'_c	Concrete cylinder compressive strength
f_y	Yield stress of steel reinforcement
h	Overall depth of slab
L	Long span length of rectangular slab
l	Short span length of rectangular slab
M	Yield bending moment per unit width of slab
M_o	Value of M with zero axial force
N	Yield axial force at mid – depth per unit width of slab
P	Uniformly distributed load per unit area
P_J	Johansen's yield line theory load
Q	Nodal force
T_o	Yield force in tensile reinforcement per unit width of slab
t	Parameter $= 0.59\ \rho\ f_y/f'_c$
w_o	Vertical deflection at center of free edge
w_o'	Value of w_o when the slab is first cracked throughout its depth.
$\dot{\varepsilon}$	Plastic axial strain rate at mid – depth of slab
$\dot{k}$	Plastic curvature rate
θ	Rotation of triangular middle surface element about the long fixed edge of the slab
$\emptyset$	Rotation of triangular middle surface element about the short fixed edge of the slab
μ	Depth of neutral axis measured from mid – depth of slab
ρ	Ratio of steel area to effective area of a slab section of unit width $= A_s/d$
φ	Angle fixing yield line patteren

Introduction

The Johansen's yield theory based on rigid – plastic approximation [1] has been proven successful in predicting the ultimate loads of reinforced concrete slabs. This ultimate load is

known as Johansen's yield line theory load and is assumed to be independent of the deflections.

Yield line load obtained by Johansen's yield line theory is found to be less than the ultimate load obtained from tests [2]. This load enhancement is due to boundary restraints and change in geometry. This phenomenon is called membrane action. Many researchers using rigid plastic analysis have been reported in the past [2-5]. These methods are able to predict the ultimate load of such slabs at zero deflection and the descending portion of the load deflection curve. However, they are unable to trace of actual load – deflection behavior. Many researchers [6-9] have looked into the actual load-deflection behavior of unrestrained and restrained reinforced concrete slabs. These analyses were carried out in three stages; elastic, elasto-plastic and plastic. The predicted load deflection relationships obtained from these analyses showed good agreement with experimental results. The same approach was adopted by Kadir [10] to predict the complete load-deflection behavior of rectangular slab with three sides simply supported and the fourth free under uniform loading. The theoretical predictions of this work are fairly comparable with the experimental results. In the present work, an attempt has been made to predict the load – deflection behavior of rectangular slabs with three edges fixed and the fourth edge is free under uniformly loading including the effect of membrane action.

Theoretical Analysis

A rectangular slab, with one long edge free and the three other edges fixed, as shown in Fig (1) is analyzed under uniformly distributed load. The slab is isotropically reinforced in the bottom face and with the same amount of reinforcement in the top face only at supports. The load – deflection relationship is idealized as shown in Fig (2). The analysis is carried out in three stages.

1- Elastic stage.
2- Elasto-plastic stage.
3- Plastic stage.

1- Elastic stage

In this stage, the slab behaves as an elastic plate. The elastic segment (OA) of the load – deflection relationship is essentially a straight line defining full elastic behavior in this region. The maximum deflection and the maximum bending moment at mid – span of unsupported side is calculated from classical plate theory [11]

$$w_{max} = \alpha_1 \frac{(1-v^2)\, PL^4}{E_c I_g} \qquad \ldots\ldots (1)$$

and $$M_{max} = \beta_1 PL^2 \qquad \ldots\ldots (2)$$

where α_1 and β_1 are deflection and bending moment coefficients, respectively.

The constants α_1 and β_1 depend on the L/l ratio and Poisson's ratio v [11]. Numerical values of α_1 and β_1 are found from Table (1). This table is a copy of the table found in Ref 11].

It can be seen from Fig (2) that the slab during this stage is relatively stiff and any increase in load is accompanied by a proportional increase in deflection.

The pre-cracking elastic region ends when first cracking appears at mid- span of the unsupported side at an intensity of load of P_{cr}. This is represented by point A in Fig (2) which can be estimated by equating M_{max} to the cracking moment M_{cr} such that

$$M_{max} = M_{cr} = \frac{f_r\, I_g}{y_t} \qquad \ldots\ldots (3)$$

A combination of Eqs (2) and (3) gives

$$P_{cr} = \frac{f_r\, I_g}{y_t\, \beta_1\, L^2} \qquad \ldots\ldots (4)$$

and when this value of load is substituted into Eq (1) the cracking deflection w_{cr} corresponding to point A will be

$$w_{cr} = \frac{\alpha_1(1-v^2)}{\beta_1}\ \frac{f_r\ L^2}{y_t\ E_c} \qquad \ldots\ldots (5)$$

By using $f_r = 0.7\sqrt{f'_c}$ and $E_c = 4700\sqrt{f'_c}$ (as recommended by ACI Code [12] and knowing that $I_g = \frac{h^3}{12}$ and $y_t = \frac{h}{2}$ Eqs (4) and (5) may be reduced to

$$P_{cr} = \frac{0.1\sqrt{f'_c}}{\beta_1} \left(\frac{h}{L}\right)^2 \qquad \ldots\ldots (6)$$

$$w_{cr} = 3 * 10^{-4} \left(\frac{\alpha_1}{\beta_1}\right)(1-v^2) \left(\frac{L}{h}\right) \qquad \ldots (7)$$

2- Elasto-plastic Stage

This stage starts from the cracking load at A to Johansen's simple yield line theory load at D, where flexural cracking occurs at the maximum bending moment regions of the slab, and there is a deviation of the load – deflection relationship from linearity.

The effect of cracking of concrete and yielding of steel is included by choosing a decreasing moment of inertia Function (I_e) analogous to that specified by ACI Code [12].

$$I_e = \frac{(P_{cr})}{(P_i)} I_g + \left[1 - \left(\frac{P_{cr}}{P_i}\right)^3\right] I_{ct} \quad \ldots\ldots(8)$$

Where P_i represents the intensity of the uniformly distributed load at the stage deflection is computed, and I_{ct} is the moment of inertia of the slab cracked transformed section per unit width,

$$I_{ct} = \frac{bd^3}{3} [k^3 + 3n\rho (1-k)^2] \quad \ldots\ldots(9)$$

Where

$$k = \sqrt{(\rho n)^2 + 2\rho n} - \rho n$$

$n = \frac{E_s}{E_c}$ and ρ is the reinforcement ratio

The load P_i can still be calculated on the elastic basis from Eq (2) by substituting M_{max}, the moment capacity of the slab section at that given stage, thus

$$P_i = \frac{M_{i,max}}{\beta_1 L^2} \quad \ldots\ldots(10)$$

Referring to Fig (2), the elasto – plastic stage is subdivided into three regions (segments) AB, BC and CD.

Region (segment) AB

The pre-cracking elastic region terminates at the initiation of the first crack and moves into region AB of the load – deflection relationship Fig (2). Most slabs lie in this region at service loads. After cracking and before yielding of reinforcement, the slab is no longer of constant stiffness, since the cracked regions have lower flexural stiffness, EI, than the un-cracked regions, and the slab is no longer isotropic, since the crack pattern may differ in the two directions. Although this violates the assumptions in the elastic theory, tests indicate that the elastic theory still predicts the moment adequately [13].

When the terminating point B is reached, the steel bars commence to yield at the maximum moment region and the moment capacity of the slab at this section is simply the yield moment M_y, which can be calculated on the basis of the stress distribution shown in Fig (3) as

$$M_y = \rho f_y d^2 (1 - \frac{k}{3}) \quad \ldots\ldots(11)$$

The corresponding load and deflection are

$$P_y = \frac{M_y}{\beta_1 L^2} \quad \ldots\ldots(12)$$

and

$$w_y = w_{cr} + \frac{\alpha_1 (1-v^2)(P_y - P_{cr}) L^4}{E_c (I_e)_y} \quad \ldots\ldots(13)$$

in which

$$(I_e)_y = (\frac{P_{cr}}{P_y})^3 I_y + \left[1 - \left(\frac{P_{cr}}{P_y}\right)^3\right] I_{ct} \quad \ldots\ldots(14)$$

Region (segment) BC

Along portion BC, the slab continues to yield and a heavy spread of cracks may be observed accompanied by inelastic compressive stress distribution of concrete until when point C is reached the section of slab at maximum moment region has reached its ultimate moment capacity (M_o) where

$$M_o = \rho f_y d^2 (1 - 0.59\rho \frac{f_y}{f'_c}) \quad \ldots\ldots(15)$$

The corresponding load and deflection are

$$P_o = \frac{M_o}{\beta_1 L^2} \quad \ldots\ldots(16)$$

and

$$w_u = w_y + \frac{\alpha_1 (1-v^2)(P_o - P_y) L^4}{E_c (I_e)_o} \quad \ldots\ldots(17)$$

in which

$$(I_e)_o = (\frac{P_{cr}}{P_o})^3 I_g + \left[1 - \left(\frac{P_{cr}}{P_o}\right)^3\right] I_{ct} \quad \ldots\ldots(18)$$

Region (segment) CD

With further load, the regions of yielding known as yield lines divide the slab into a series of trapezoidal or/and triangular elastic plates as shown in Fig (4). The load corresponding to this stage of behavior can be estimated by using the yield – line theory analysis [1]. The Johansen's yield line theory load P_J (corresponding of point D) for mode (1) is determined following the principle of virtual work method as follows:
The positive yield line is given a unit displacement and the internal work is calculated as

$$I.W. = 2M_o\left[4\left(\frac{l}{L}\right)+\frac{1}{\eta\,(\frac{l}{L})}\right]$$

The external work done can be thought of as being the uniform load multiplied by the volume swept out by the slab segments when displaced, thus

$$E.W. = \frac{P_J}{6}\left(\frac{l}{L}\right)L^2\,[3-\eta]$$

Equating the external and internal works gives

$$P_J = \frac{12\,M_o\left[4\,(\frac{l}{L})^2\eta+1\right]}{(\frac{l}{L})^2L^2\,\eta\,(3-\eta)} \qquad \ldots\ldots(19)$$

The value of η corresponding to the least value of P_J is obtained by equating the derivative of Eq (19) to zero, gives

$$\eta = \frac{1}{4\,(\frac{l}{L})^2}\left[\sqrt{1+12\,(\frac{l}{L})^2}-1\right] \qquad \ldots\ldots(20)$$

Substituting η from Eq (20) into Eq (19) gives the least P_J as

$$P_J = \frac{48\,M_o}{L^2}\left[\sqrt{3+\frac{1}{4\,(\frac{l}{L})^2}}-\frac{1}{2(\frac{l}{L})}\right]^2 \qquad \ldots\ldots(21)$$

The deflection at D is calculated as follows:
Changes that occur in support conditions along the fixed sides due to the formation of the negative yield lines at Johansen's load is to be considered. This is done by changing the deflection coefficient α_1 in Eq (1) to be the average of the cases of simply supported and fixed supports as

$$w_J = w_o + \alpha_{1m}\frac{(P_J-P_o)L^4}{E_c\,(I_e)_J} \qquad \ldots\ldots(22)$$

where α_{1m} = modified deflection coefficient

and

$$(I_e)_J = (\frac{P_{cr}}{P_J})^3\,I_g + \left[1-\left(\frac{P_{cr}}{P_J}\right)^3\right]I_{ct} \qquad \ldots\ldots(23)$$

3- Third Stage (plastic Stage)

In this stage of analysis, the crucial effect of compressive membrane action in the slab is considered.
The following assumptions are made in an attempt to determine the effect of membrane action in isotropically reinforced rectangular slabs with fixed supports along three edges and free along the fourth edge.

1- Plane sections before bending remain plane after bending, i.e., the strain distribution across the depth of a section is linear.
2- The materials are rigid – perfectly plastic.
3- At the yield section, the steel has yielded and the compressed concrete has reached its ultimate strength. The stress distribution of the concrete is assumed to the shape of an equivalent rectangular block as defined by ACI code. The strength of concrete in tension is neglected.
4- The form of failure is determined by the yield – line method and is made of straight yield lines with a single yield line running into both corners, i.e. corner effects are neglected.

Analysis

A rectangular rigid plastic concrete slab with three edges fixed in and the fourth edge free, carrying a uniformly distributed load is considered, isotropically reinforced in the bottom face only at center and with the same amount of reinforcement in the top face only at supports is assumed. The slab yields under the simultaneous action of a bending moment M and a compressive axial force N acting at the slab mid – depth Fig (3).

Referring to the stress distribution at ultimate stage shown in Fig (3),

$$N = 0.85 f'_c a - A_s f_y \quad \ldots\ldots(24)$$

$$M = 0.85 f'_c a \left(\frac{h}{2} - \frac{a}{2}\right) + A_s f_y \left(d - \frac{h}{2}\right) \quad \ldots\ldots(25)$$

A combination of equations (24) and (25) leads to the following non-dimensional yield criterion:

$$\frac{M}{M_o} = 1 + \alpha \left(\frac{N}{T}\right) - \beta \left(\frac{N}{T}\right)^2 \quad \ldots\ldots(26)$$

Where M_o: is as given by Eq (15)

$$T_o = A_s f_y = \rho\, d\, f_y$$

$$\alpha = \frac{\frac{1}{2}\frac{h}{d} - 1.18\,\rho\,\frac{f_y}{f'_c}}{1 - 0.59\,\rho\,\frac{f_y}{f'_c}}$$

$$\beta = \frac{0.59\,\rho\,\frac{f_y}{f'_c}}{1 - 0.59\,\rho\,\frac{f_y}{f'_c}}$$

If the yield criterion is denoted by a function f, the ratio of the plastic axial strain rate $\dot{\varepsilon}$ to the plastic curvature rate $\dot{k}$ according to plastic potential flow rule [5] must be

$$\frac{\dot{\varepsilon}}{\dot{k}} = \mu = \frac{\partial f/\partial N}{\partial f/\partial M} = \frac{\frac{\alpha}{T} - 2\beta\frac{N}{T_o}}{\frac{1}{M_o}}$$

From which

$$\frac{N}{T} = \left(\frac{\alpha}{2\beta}\right) - \frac{\mu}{2\beta}\frac{T_o}{M_o} \quad \ldots\ldots(27)$$

Yield Mechanism and Compatibility Equations

An initial collapse mechanism of the type shown in Fig (4 b) is considered and assumed to be preserved at large deflections. This mode was chosen to simplify the geometry of the yield mechanism. If the vertical deflection at mid – point of the free edge is w, the corresponding rotations of the triangular middle surface elements (Fig 5) relative to the supporting edges are θ and $\emptyset$ respectively. These plastic rotations are related to the plastic axial elongations e_1 at sagging yield lines and e_2 and e_3 at hogging yield lines according to the following compatibility equations:

Sec. 1-1

$$2\,e_3 + 2\,x\cos\emptyset + 2\,e_1\sin\varphi + L - 2x = L$$

For small angle of $\emptyset$, $\cos\emptyset = 1 - \frac{\emptyset^2}{2}$

$$e_3 + e_1\sin\varphi = x\,.\frac{\emptyset^2}{2}$$

Since $y\,\theta = x\,\emptyset$

$$e_3 + e_1\sin\varphi = \frac{x}{2}\,(\tan^2\varphi).\theta^2$$

$$e_3 = x\,\frac{\theta^2}{2}\tan^2\varphi - e_1\sin\varphi \quad \ldots\ldots(28)$$

Sec. 2-2

$$e_2 + y\cos\theta + e_1\cos\varphi + l - y = l$$

For small angle of θ, $\cos\theta = 1 - \frac{\theta^2}{2}$

$$e_2 = y\,\frac{\theta^2}{2} - e_1\cos\varphi \quad \ldots\ldots(29)$$

From Eqs (28) and (29)

$$\frac{e_2}{e_3} = \cot\varphi \quad \ldots\ldots(30)$$

From Eq (28), when $x = \frac{L}{2}$, $e_1 = e_o$

$$e_3 = \frac{L}{2}\,\frac{\theta^2}{2}\,tan^2\,\varphi - e_o\sin\varphi$$

From Eq (30)

$$e_3 = e_2\tan\varphi$$

$$\therefore e_2\tan\varphi = \frac{L}{2}\,\frac{\theta^2}{2}\,tan^2\,\varphi - e_o\sin\varphi$$

$$\therefore e_2 = \frac{L}{4}\,\theta^2\tan\varphi - e_o\cos\varphi \quad \ldots\ldots(31)$$

From Eq (31) and (29)

$$e_1\cos\varphi = e_o\cos\varphi - \frac{L}{4}\theta^2\tan\varphi + y\,\frac{\theta^2}{2}$$

Differentiate w.r.t. θ

$$\frac{de_1}{d\theta}\cos\varphi = \frac{de_o}{d\theta}\cos\varphi - \frac{L}{2}\,\theta\tan\varphi + y\,\theta$$

From strain distribution at sagging yield lines (Fig 6)

$$\frac{de_1}{\mu_1} = d\gamma$$

$$\therefore\quad \mu_1 = \frac{de_1}{d\gamma} = \frac{de_1}{d\theta.\sec\varphi} = \frac{de_1}{d\theta}\cos\varphi$$

$$\mu_o = \frac{de_o}{d\theta}\cos\varphi$$

$$\emptyset = \frac{w_o}{\frac{L}{2}} = \frac{2w_o}{L}$$

$$\emptyset = \tan\varphi\,.\,\theta \qquad \text{Fig (6)}$$

$$\therefore\quad \frac{2w_o}{L} = \tan\varphi\,.\,\theta$$

$$\therefore\quad \theta = \frac{2w_o}{L\tan\varphi}$$

$$\frac{de_1}{d\theta}\cos\varphi = \frac{de_o}{d\theta}\cos\varphi - \frac{L}{2}\,\theta\tan\varphi + y\,\theta$$

$$\mu_1 = \mu_o + \theta\left[y - \frac{L}{2}\tan\varphi\right]$$

$$\therefore\quad \mu_1 = \mu_o + \frac{2w_o}{L\tan\varphi}\left[y - \frac{L}{2}\tan\varphi\right] \qquad \ldots\ldots(32)$$

From strain distribution at hogging yield lines

$$\mu_2 = \frac{de_2}{d\theta}$$

$$\mu_3 = \frac{de_3}{d\emptyset} = \frac{de_3}{d\theta.\tan\varphi} = \cot\varphi\,.\,\frac{de_3}{d\theta}$$

From Eq (31)

$$e_2 = \frac{L}{4}\,\theta^2\tan\varphi - e_o\cos\varphi$$

$$\mu_2 = \frac{de_2}{d\theta} = \frac{L}{2}\,\theta\tan\varphi - \frac{de_o}{d\theta}\cos\varphi$$

$$= \frac{L}{2} * \frac{2w_o}{L\tan\varphi}\,.\,\tan\varphi - \mu_o$$

$$\mu_2 = w_o - \mu_o = \mu_3 \qquad \ldots\ldots(33)$$

Eq (32) define the depth of the neutral axis along the sagging yield lines whereas Eq (33) define the neutral axis depth along the hogging yield lines at the slab periphery.

Horizontal Equilibrium Equations

The only unknown in Eqs (32) and (33) for a given maximum deflection w_o is μ_o and this may be determined by considering the horizontal equilibrium of either elements (1) or (2) in Fig (7). Due to symmetry arguments, there can no-inplane shear force acting on the slab along the yield lines.

Considering element (2) and resolving forces perpendicular to the fixed edge of element (2) in Fig (7) gives:

$$\int N_1.\sin\varphi\ ds - N_3\,l = 0$$

but $ds = \frac{dy}{\sin\varphi}$

$$\therefore\quad T_o\int_0^l \frac{N_1}{T_o}dy - T_o\frac{N_3}{T_o}l = 0$$

$$\therefore\quad \int_0^l \frac{N_1}{T_o}dy - \frac{N_3}{T_o}l = 0 \qquad \ldots\ldots(34)$$

The values of the membrane forces N_1 and N_3 acting perpendicular to the yield lines are obtained by substituting the values of μ_1 and μ_3 defined by Eqs (32) and (33) each at a time into Eq (27), which gives

$$\frac{N_1}{T_o} = A_1 - B_1(\frac{y}{l} - 1)$$

$$\frac{N_2}{T_o} = \frac{\alpha}{\beta} - A_1 - B_1$$

Where

$$A_1 = \frac{\alpha}{2\beta} - \frac{\mu_o}{2\beta}\frac{T_o}{M_o}$$

$$B_1 = \frac{w_o}{2\beta}\frac{T_o}{M_o}$$

Reducing Eq (34) gives

$$2A_1 + \frac{3B_1}{2} - \frac{\alpha}{\beta} = 0$$

$$\mu_o = \frac{3}{4} w_o \qquad \ldots\ldots (35)$$

The limiting deflection $w_o{}'$ for which Eq (35) is valid is obtained when $\mu_o = {}^{h}/_{2}$

$$\frac{h}{2} = \frac{3}{4} w_o{}'$$

$$\therefore \quad \frac{w_o{}'}{h} = \frac{2}{3} \qquad \ldots\ldots (36)$$

Using the expression of the limiting deflection $w_o{}'$ given by Eq (36), the value of μ_o represented by Eq (35) may be written in the following form

$$\mu_o = \frac{w_o}{w_o{}'} \frac{h}{2} \qquad \ldots\ldots (37)$$

It is apparent from this equation that at zero deflection, $\mu_o = 0$ and therefore the neutral axis of the slab section coincides with mid – depth axis. This indicates a concrete compression block extending as for as half the slab thickness. With increasing deflection, the neutral axis at the central region of the slab shifts upward, until when w_o reaches $w_o{}'$ the concrete block vanishes and the neutral axis touches the slab top surface (full depth cracking).

Yield moment and axial forces

The axial forces can be determined by introducing the value of μ_o from Eq (35) into Eq (32) and (33) with use of Eq (27) the results will be

$$\frac{N_1}{T_o} = \frac{\alpha}{2\beta} - \frac{w_o}{8\beta} \frac{T_o}{M_o} \left(4\frac{y}{l} - 1\right) \qquad \ldots\ldots (38)$$

and

$$\frac{N_2}{T_o} = \frac{N_3}{T_o} = \frac{\alpha}{2\beta} - \frac{w_o}{8\beta} \frac{T_o}{M_o} \qquad \ldots\ldots (39)$$

Substituting the expressions for $\frac{N}{T_o}$ into Eq (26) gives the corresponding equations for the yield moments

$$\frac{M_1}{M_o} = \left(1 + \frac{\alpha^2}{4\beta}\right) - \frac{1}{\beta} \left(\frac{w_o}{8}\right)^2 \left(\frac{T_o}{M_o}\right)^2 \left(\frac{4y}{l} - 1\right)^2 \ldots (40)$$

$$\frac{M_2}{M_o} = \frac{M_3}{M_o} = \left(1 + \frac{\alpha^2}{4\beta}\right) - \frac{1}{\beta} \left(\frac{w_o}{8}\right)^2 \left(\frac{T_o}{M_o}\right)^2 \qquad \ldots (41)$$

Yield loads

Having expressed the values of the axial forces $\frac{N}{T_o}$ and the yield moments M/M_o in terms of maximum deflection of the slab w_o, the yield loads corresponding to any maximum deflection can now be found by considering the equilibrium of the slab elements. To account for any vertical shear, nodal forces Q are introduced at the intersection of the sagging yield line with the free edge (see Fig 8), such that the summation of these forces at the junction of the yield lines is zero.

Moment Equilibrium of the Rigid Triangular Element (abc)

Referring to the Fig (8), by taking moments about the mid – depth of the slab fixed edge *ab*, the following equilibrium equation is obtained

$$\sum M_{ab} = 0$$

$$\boldsymbol{P * \frac{1}{2} L\, l * \frac{l}{3} + 2 \int_0^{l \csc\varphi} N_1\, ds \cos\varphi \,.\frac{y}{l} w_o - 2 \int_0^{l \csc\varphi} M_1\, ds \cos\varphi - M_2 L - Ql = 0}$$

But $ds = \frac{dy}{\sin\varphi}$

$$\frac{PLl}{6} + w_o \frac{L}{l^3} \int_0^l N_1\, y\, dy - \frac{L}{l^2} \int_0^l M_1\, dy - M_2 \frac{L}{l} = \qquad \ldots (42)$$

Moment Equilibrium of the Rigid Triangular Element (acd)

$$P * \left(\frac{1}{2} * \frac{L}{3} l\right) * \frac{L}{6} + \int_0^{l \csc\varphi} N_1\, ds \sin\varphi \,.\frac{y_o}{l} w_o - \int_0^{l \csc\varphi} M_1\, ds \sin\varphi - M_3 l + \frac{Q}{2} * \frac{L}{2} = 0$$

substituting $ds = \frac{d_y}{sin\,\varphi}$

$$\therefore \quad \boldsymbol{\frac{-PLl}{6} - \frac{4 w_o}{L\, l} \int_0^l N_1\, y\, dy - \frac{4}{L} \int_0^l M_1\, dy - 4 \frac{l}{L} M_3 = Q} \qquad \ldots\ldots (43)$$

The nodal force Q can be eliminated by equating Eqs (42) and (43) which give

$$\therefore \quad \boldsymbol{\frac{PLl}{3\left(\frac{L}{l^2} + \frac{4}{L}\right)} + \frac{w_o T_o}{l} \int_0^l \frac{N_1}{T_o}\, y\, dy - M_o \int_0^l \frac{M_1}{M_o}\, dy - M_o l \frac{M_3}{M_o} = \cdots (44)}$$

Substituting N_1, M_1 *and* M_3 given by Eqs (38), (40) and (41) into Eq (44) gives

$$\therefore \quad \frac{PLl}{3\left(\frac{L}{l^2}+\frac{4}{L}\right)}+\frac{w_o T_o\, l}{4\beta}\left(\alpha-\frac{5w_o}{12}\frac{T_o}{M_o}\right)-M_o l\left[1+\frac{\alpha^2}{4\beta}-\frac{9}{4\beta}\left(\frac{w_o}{8}\right)^2\left(\frac{T_o}{M_o}\right)^2\right] - M_o l\left[1+\frac{\alpha^2}{4\beta}-\frac{1}{\beta}\left(\frac{w_o}{8}\right)^2\left(\frac{T_o}{M_o}\right)^2\right] = 0 \quad \ldots\ldots(45)$$

The Johansen's yield line theory load for the slab is

$$P_J = \frac{6\,M_o}{L}\left(\frac{L}{l^2}+\frac{4}{L}\right) \qquad \ldots\ldots(46)$$

Dividing Eq (45) by P_J and Reducing gives

$$\frac{P}{P_J} = 1+\frac{\alpha^2}{4\beta}-0.125\frac{\alpha}{\beta}\frac{T_o}{M_o}w_o+0.0267\frac{1}{\beta}\left(\frac{T_o}{M_o}\right)^2 {w_o}^2 \ldots(47)$$

If the expressions of α_1, β, T *and* M_o are introduced, Eq (47) will have the following form

$$\frac{P}{P_J} = 1+\frac{\left(\frac{1}{2}\frac{h}{d}-2t\right)^2}{4t(1-t)}-0.125\frac{\frac{1}{2}\frac{h}{d}-2t}{t(1-t)}\left(\frac{w_o}{d}\right)+0.0267\frac{1}{t(1-t)}\left(\frac{w_o}{d}\right)^2 \quad \ldots(48)$$

Where $t = 0.59\,\rho\,\frac{f_y}{f'_c}$

In Eq (48), the effect of rectangularity $\left(\frac{L}{l}\right)$ on the load- deflection behavior of rectangular slabs with three sides fixed and the fourth is free, is included in the load term P_J . Graphical representation of Eq (48) is given in Fig (9). The figure shows the possible enhancements in the load carrying capacity above the Johansen load due to the effect of variation in the percentage of reinforcement ρ and the slab deflection.

It is apparent from this analysis that due to compressive membrane action, rectangular R.C slabs with three sides fully restrained and the fourth is free, can carry loads far beyond those of Johansen's simple yield line theory. The reserves in strengths are found to be more pronounced in lightly reinforced slabs (Fig 9).

The assumption of rigid-perfectly plastic behavior of R.C. rectangular slabs with three edges fully restrained against rotation and horizontal translation implies that the maximum yield load is attained at zero deflection. Therefore, from Eq (47);

$$\frac{P_{mi}}{P_J} = 1+\frac{\alpha^2}{4\beta} \qquad \ldots\ldots(49)$$

where P_{mi} = ideal maximum ultimate load including compressive membrane action.

It is worth re-emphasizing here that the enhancement factor given by Eq (49) is only idealized since it is based on assuming that the slab behaves in a rigid-perfectly plastic manner. This implies that the ultimate load, which is many times greater than Johansen's yield line theory load and corresponds to zero deflection according to Eq (47), is somewhat exaggerated. If elastic strains, for instance, has been introduced in the analysis the value of the ultimate load would have reduced, and will be given as

$$\frac{P_{ma}}{P_J} = \mathcal{R}\left(1+\frac{\alpha^2}{4\beta}\right) \qquad \ldots\ldots(50)$$

where P_{ma} = actual maximum ultimate load including compressive membrane action.

$\mathcal{R}$ = reduction factor

It is suggested that a reduction factor $\mathcal{R} = 0.75$ could be used in practice [2]

The deflection w_{ma} corresponding to P_{ma} is obtained from Eq (48) as

$$\frac{w_{ma}}{d} = \frac{-B-\sqrt{B^2-4AC}}{2A} \qquad \ldots\ldots(51)$$

where

$A = 0.0267/t\,(1-t)$

$B = -0.125\left(\frac{1}{2}\frac{h}{d}-2t\right)/t(1-t)$

$C = \frac{1-\mathcal{R}}{4}\left(\frac{1}{2}\frac{h}{d}-2t\right)^2$

$C = (1-\mathcal{R})\left[1+\frac{\left(\frac{1}{2}\frac{h}{d}-2t\right)^2}{4t\,(1-t)}\right]$

$t = 0.59\,\rho\,\frac{f_y}{f'_c}$

Summary of the Analysis

A complete load-deflection diagram for a rectangular slab with three edges fixed and fourth edge free can be constructed with reference to Fig (2) as follows

1. The values of the coordinates of the points A, B, C, D, E and F are calculated using the appropriate equation as indicated below.

Point	Eq. no. used to evaluate the	
	absesa (deflection)	ordinate (Load)
A	7	6
B	13	12
C	17	16
D	22	21
E	51	50
F	36	48

2. The referred points O, A, B, C, D, E and F are connected by straight lines.

Illustration of proposed method

To illustrate the proposed method, a hypothetical R.C rectangular slab with three edges fixed and the fourth edge free under uniformly distributed load is considered. The slab is isotropically reinforced in the bottom face and with the same amount of reinforcement in the top face only at supports and having the following properties

$L = 1000\,mm,\ \ l = 600\,mm,\ \ h = 30\,mm,\ \ d = 26\,mm,\ \ \rho = 0.25\,\%,\ f'_c = 21\,MPa$

$f_y = 414\,MPa,\ \ v = 0.15,\ \ E_s = 200000\,MPa.$

1- The values of the coordinates of the points A, B, C, D, E and F are calculated using the appropriate equation as indicated previously. The results are as shown.

Point	Deflection, W_o (mm)	Load, P kN
A	0.79	12.3
B	1.76	19.5
C	1.86	20.22
D	5.84	38.7
E	15.6	64.2
F	25.84	58.85

2- The referred points are connected by straight lines to obtain a complete load deflection relation similar to that of Fig (2). This is shown in Fig (10).

3- The predicted load-deflection curve Fig (10) is very comparable in shape with typical experimental load-deflection curves of restrained slabs. Unfortunately, there is no experimental data available in hand to show the discrepancies.

4- As the load is increased from O to E, the slab behavior is initially elastic and then become inelastic at the critical sections at higher loads until at E the yield line pattern for the slab is fully developed. When the ultimate load at E is reached the compressive forces at the surrounds become maximum and there after decline as the deflection increases resulting in a decrease in the value of the load. Comparing the predicted actual ultimate load with that of ACI Code and yield line theory, there are respectively,218% and 66% increase in the ultimate load for this particular case.

Summary and Conclusions

A method has been proposed to predict the load-deflection behavior of R.C. rectangular slabs with three edges fixed and the fourth edge free under uniformly distributed loading.

The main conclusions to be drawn from the present study are:

1- The predicted load-deflection relationships are very comparable in shape with the typical experimental load-deflection curves of restrained slabs.

2- The slabs have ultimate loads which are far in excess of that indicated by Johansen's yield line theory and ACI Code due to development of compressive membrane forces.

3- The enhancement in ultimate load above Johansen's load is more pronounced in lightly reinforced slabs.

سلوكية الحمل والاود للبلاطات الخرسانية المسلحة المستطيلة الشكل بثلاثة حافات مثبتة والرابعة حرة تحت تاثير الحمل المنتظم

د . علي فليح حسن – استاذ مساعد
جامعة دهوك –كلية الهندسة– قسم الهندسة المدنية

المستخلص :
يقدم البحث طريقة لايجاد العلاقة المتكاملة بين الحمل المنتظم والاود للبلاطات الخرسانية المسلحة المستطيلة الشكل بثلاثة حافات مثبتة والرابعة حرة تحت تاثير الحمل المنتظم. تغطي الطريقة المقترحة المراحل الثلاثة الرئيسية في التحليل والمتمثلة بمراحل المرونة،اللامرونة واللدونة . في مرحلة المرونة تم استخدام نظرية الالواح التقليدية لاستنباط العلاقة بين الحمل والاود لحد حمل التشقق . المرحلة الثانية تمثل مرحلة المرونة– اللامرونة وتبدأ هذة المرحلة من حمل التشقق الى حمل نظرية الخضوع. تم في هذة المرحلة الاخذ بنظر الاعتبار حالة التشقق للخرسانة والخضوع لحديد التسليح وذلك بتعديل جساءة الانحناء وكذلك التغير في حالة الاسناد للحافات المثبتة نتيجة تكوين خطوط خضوع عند حمل نظرية الخضوع. في مرحلة اللدونة وبالأعتماد على نظرية سيولة الأجسام الجاسئه اللدنة ،تم استخدام طريقة لاحتساب الحمولة القصوى وايجاد التصرف اللدن اخذا بنظر الاعتبار التأثيرات المهمة للقوى الغشائية المتولدة في مستوى البلاطة على طول خطوط الخضوع أثناء هطول البلاطة . أستخدمت قوانين الاتزان والتوافق لعناصر البلاطة المشوهة لأشتقاق.

الكلمات المفتاحية : فعل الضغط الغشائي ، نظرية اللدونة، المقاومة القصوى ، خطوط الخضوع.

References

1- Johansen, K.W., "Yield Line Theory", Cement and Concrete Association, London, 1962, pp.181.

2- Wood, R.H., "Plastic and Elastic Design of Slabs and Plates", Thames and Hudson, London, 1961.
3- Park, R., "Ultimate Strength of Rectangular Concrete Slabs Under Short-Term Uniform Loading with Edges Restrained Against Lateral Movement", Proceeding of the Institution of Civil Engineers, Vol. 28, June, 1964, pp.125-150.
4- Morley, C.T, "Yield Line Theory for Restrained Slabs at Moderately Large Deflections". Magazine of Concrete Research. Vol. 19 No. 61, December 1967, pp. 211-222.
5- Al-Hassani, H.M, "Ultimate Strength of Clamped R.C Rectangular Slabs under Combined Bending and Membrane Action", Journal of Engineering and Technology, Vol. 12, No. 4, 1993, pp.71-104.
6- Desayi, P., and Kulkarni, A.B," Load- Deflection Behavior of Restrained Concrete Slabs ", Journal of Structural Division, ASCE, Vol. 103, No. ST2, Feb.1977.
7- Hassan, A.F," Load- Deflection Behavior of Unrestrained R.C. Rectangular Slabs", Technical Journal of the Foundation of Technical Institutes, 1994.
8- Al-Hassani, H.M. and Hassan, A. F," Pre-and Post-Cracking Behavior of Unrestrained Reinforced Concrete Polygonal Slabs", Journal of Engineering and Technology. 18,NO.4,1999.
9- Hassan, A.F." Load-Deflection Relationship for Clamped-Horizontally Restrained Polygonal Slabs" Sulaimani Journal for Engineering Sciences, Vol.4, No.5, Nov.2017.
10- Kadir, S.S." Behavior of Unrestrained Rectangular Reinforced Concrete Slabs under Uniformly Distributed Loads" MSc thesis, University of Duhok,2001
11- Timoshenko, S.P., and Krieger, S.W., "Theory of Plates and Shells", McGraw-Hill Book Company, Inc., New York, N.Y., 1959.
12- Building Code Requirements for Reinforced Concrete, ACI 318-14, American Concrete Institute, Detroit, Mich., 2014.
13- MacGregor, J.G. and Wight, J.K, "Reinforced Concrete Mechanics and Design", 4th ed., Pearson Prentice Hall, 2005, pp.402.
14- Al-Hasseni, H.M., Behavior of Axially Restrained Concrete Slabs", Ph.D. thesis, University College London, England, 1978.
15- Desayi, p., and Kulkarni, A.B, "Load – Deflection Behavior of Restrained Concrete Slabs", Journal of the Structural Division, ASCE, Vol.103 No ST2, Feb, 1977.

Table 1 : Deflection and bending moment coefficients of uniformly rectangular plates with edges fixed and the fourth edge free (Fig.1) * (by researcher)

$\frac{L}{l}$	α_1	β_1
0.60	0.00271	0.0336
0.70	0.00292	0.0371
0.80	0.00308	0.0401
0.90	0.00323	0.0425
1.00	0.00333	0.0444
1.25	0.00345	0.0467
1.50	0.00335	0.0454

* From Ref. [6]

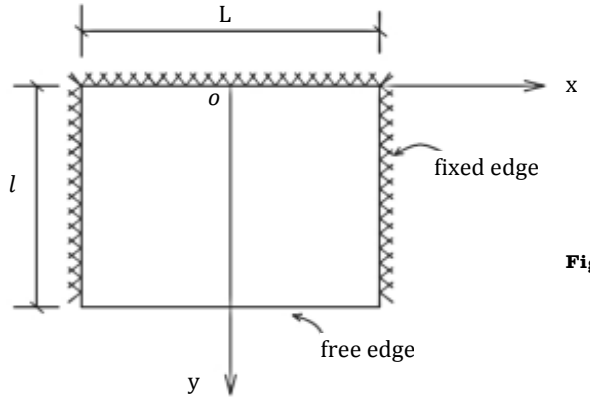

Fig. 1: Rectangular slab with three edges fixed and the fourth edge free. (by researcher)

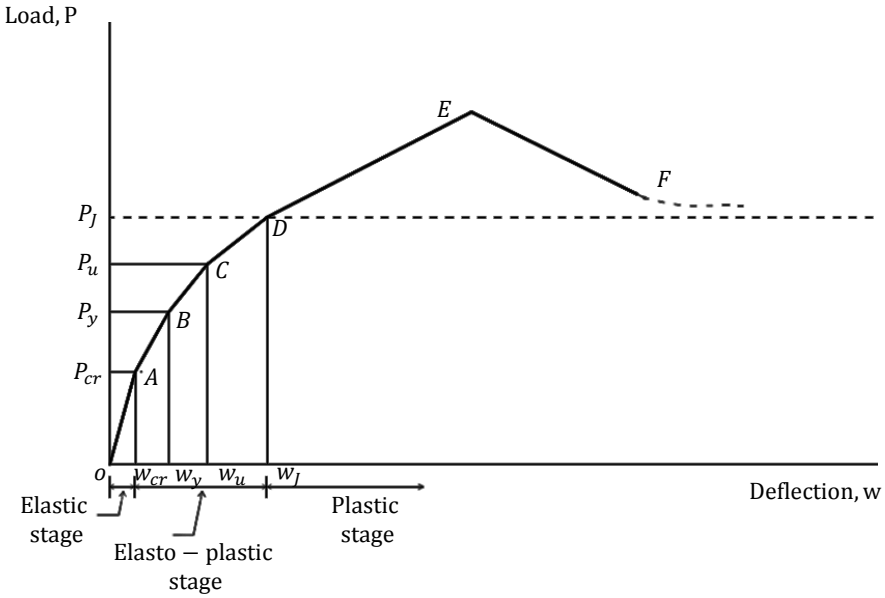

Fig. 2 : Idealized Load-deflection curve of a R.C rectangular slab with three edges fixed and the fourth edge free [8,10]

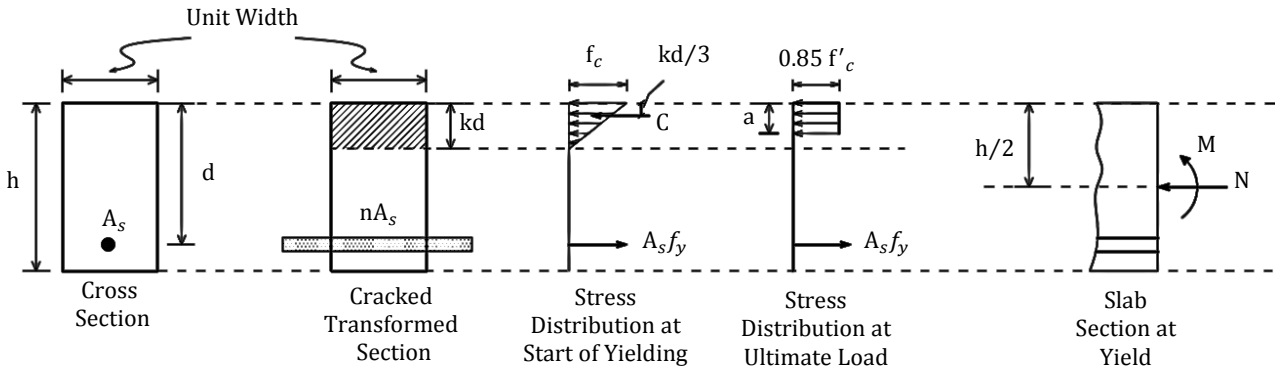

Fig. 3 : Stress Distribution on Slab Section. ((by researcher)

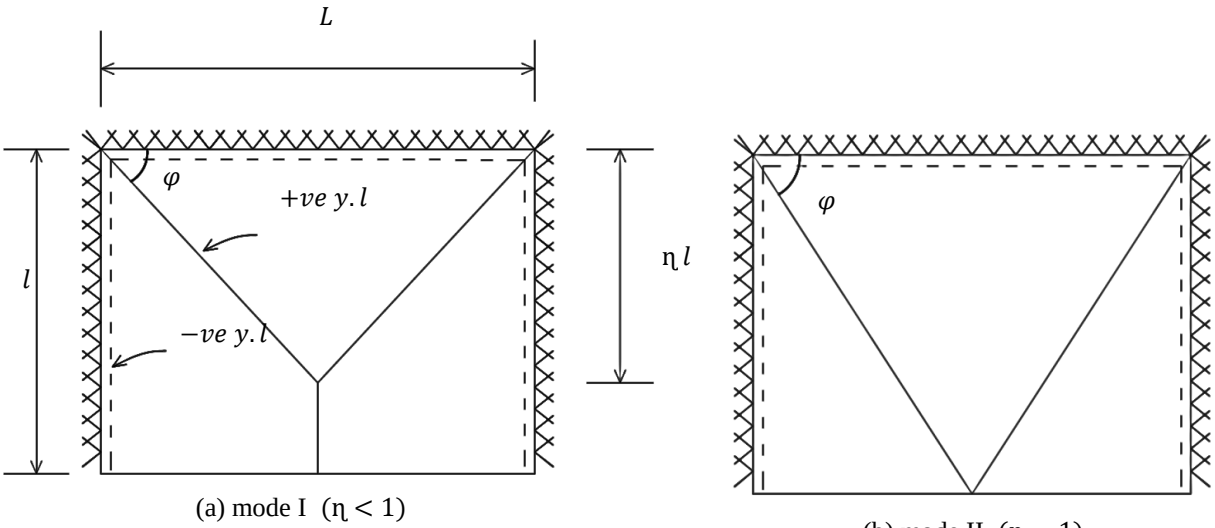

(a) mode I ($\eta < 1$)

(b) mode II ($\eta = 1$)

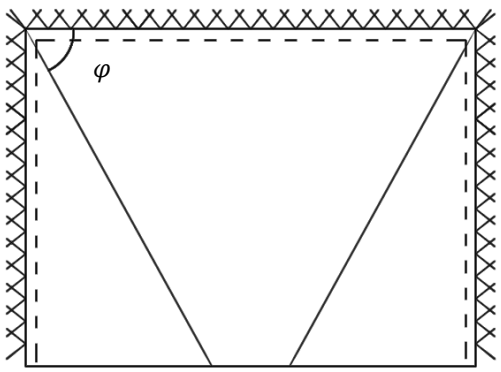

(c) mode III ($\eta > 1$)

Fig. 4 : Yield line patterns (mechanisms) for the rectangular slab with three edges fixed and the fourth edge free. (By Researcher)

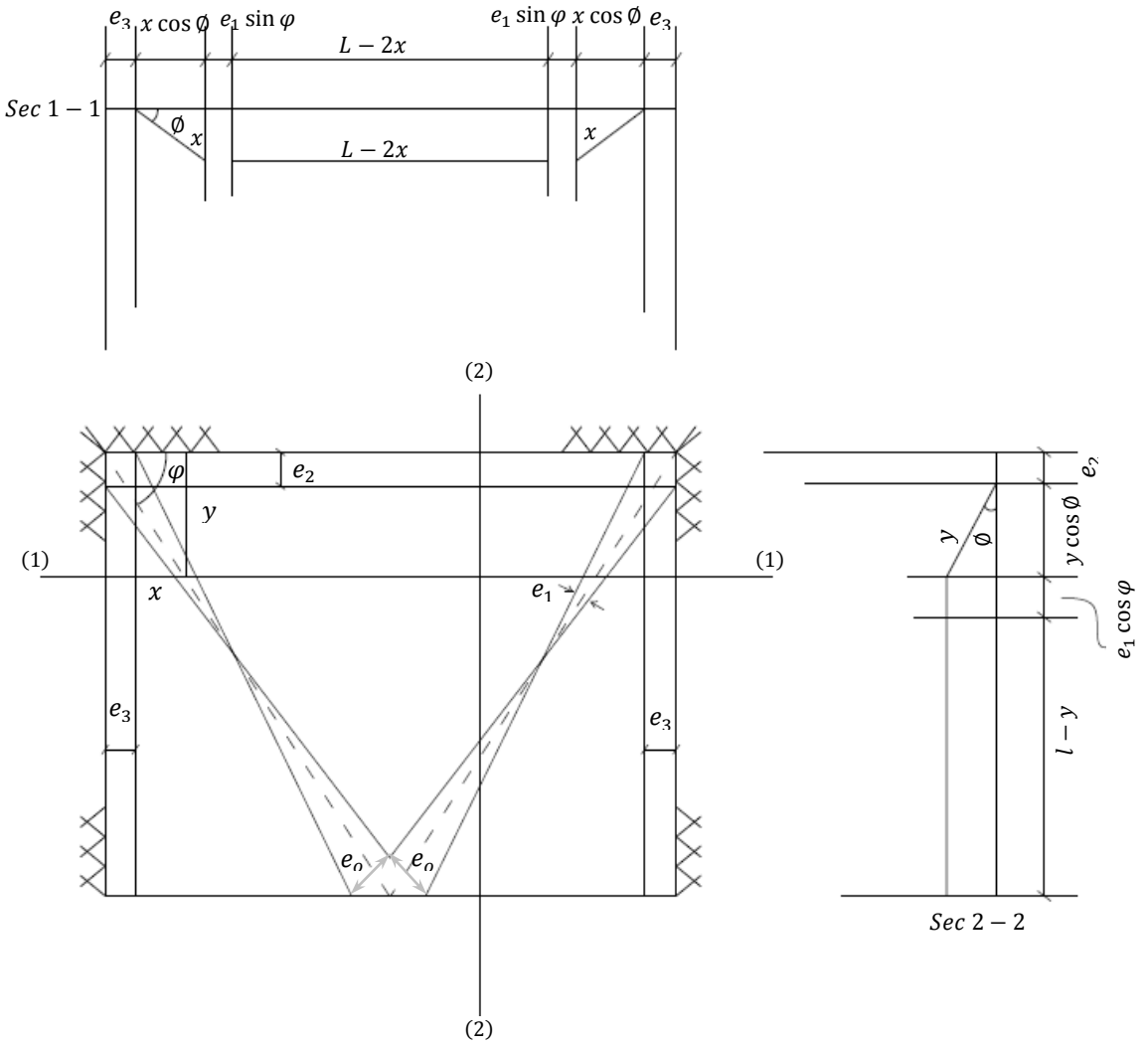

Fig. 5 : Deformation of the rigid mechanism. (by researcher)

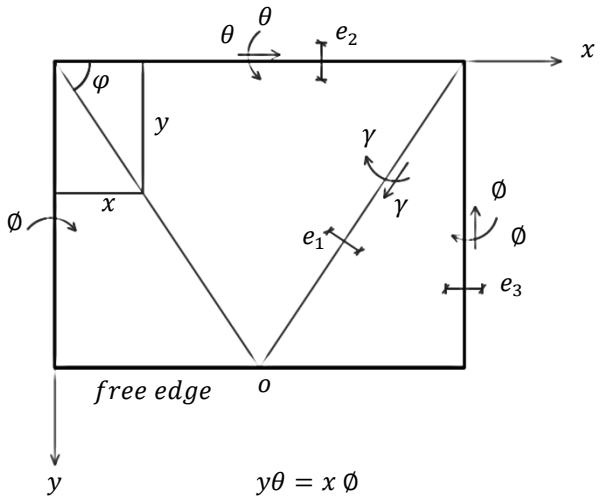

$$y\theta = x\,\emptyset$$

$$or \quad \emptyset = \frac{y}{x}\,\theta = \tan\varphi\ .\theta$$

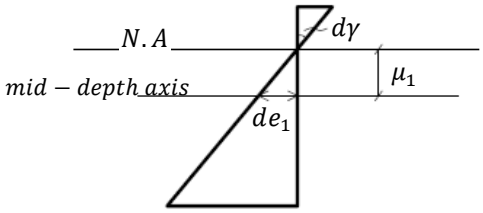

Strain distribution at sagging lines

$$d\gamma = d\theta\cos\varphi + d\emptyset\sin\varphi$$
$$= d\theta\cos\varphi + d\theta\tan\varphi\sin\varphi$$
$$= d\theta\sec\varphi$$

$$\mu_1 = \frac{de_1}{d\gamma} = \frac{de_1}{d\theta\sec\varphi} = \cos\varphi\ .\frac{de_1}{d\theta}$$

$$\mu_o(concluded\ from\ \mu_2 = \cos\varphi\ .\frac{de_o}{d\theta}$$

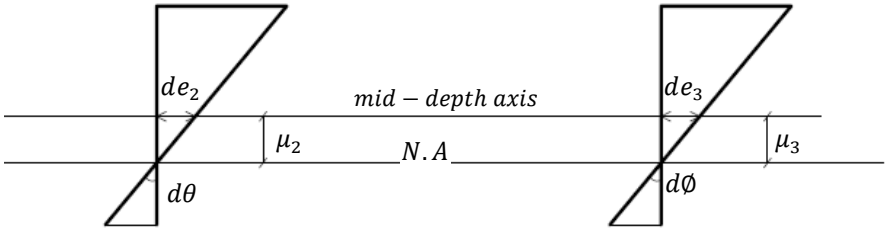

$$\mu_2 = \frac{de_2}{d\theta} \qquad \mu_3 = \frac{de_3}{d\emptyset} = \frac{de_3}{d\theta\tan\varphi} = \cot\varphi\ .\frac{de_3}{d\theta}$$

Fig. 6 : Strain distribution at sagging and hogging yield lines. (by researcher)

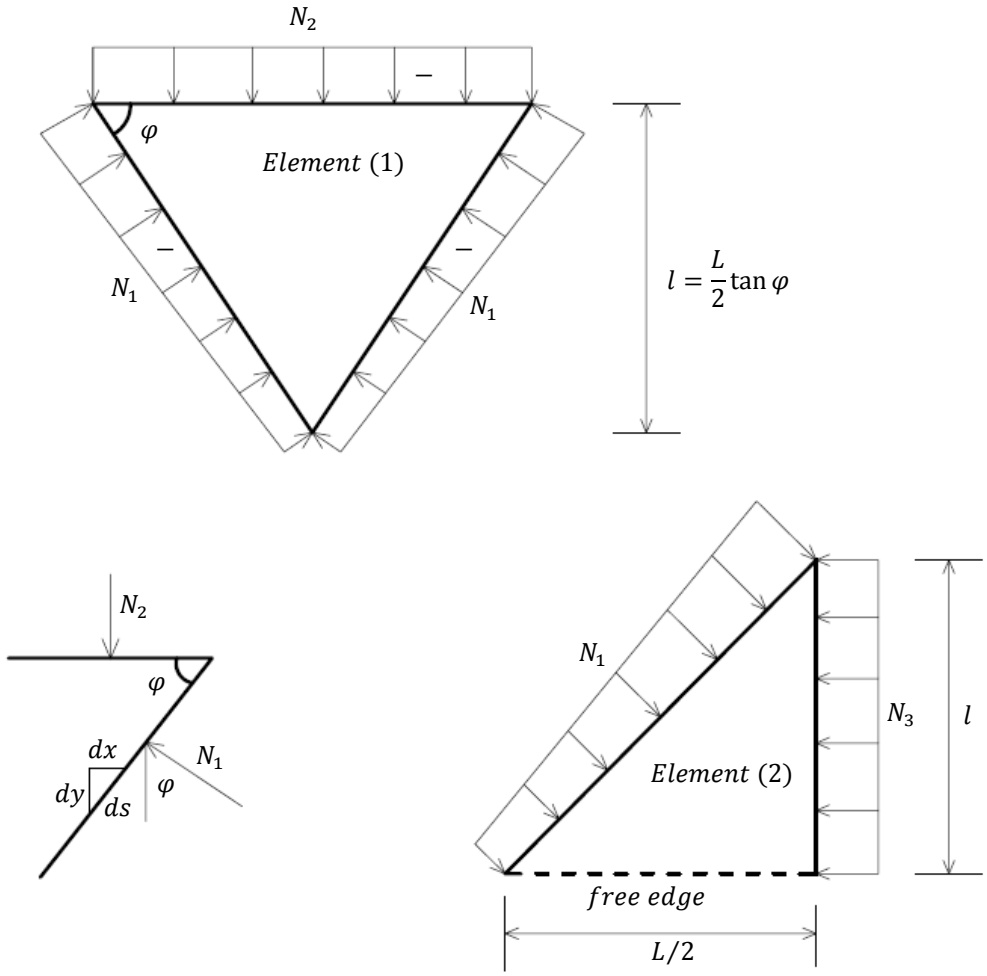

Fig. 7 : Horizontal forces on slab elements before the formation of a pure tensile membrane. (by researcher)

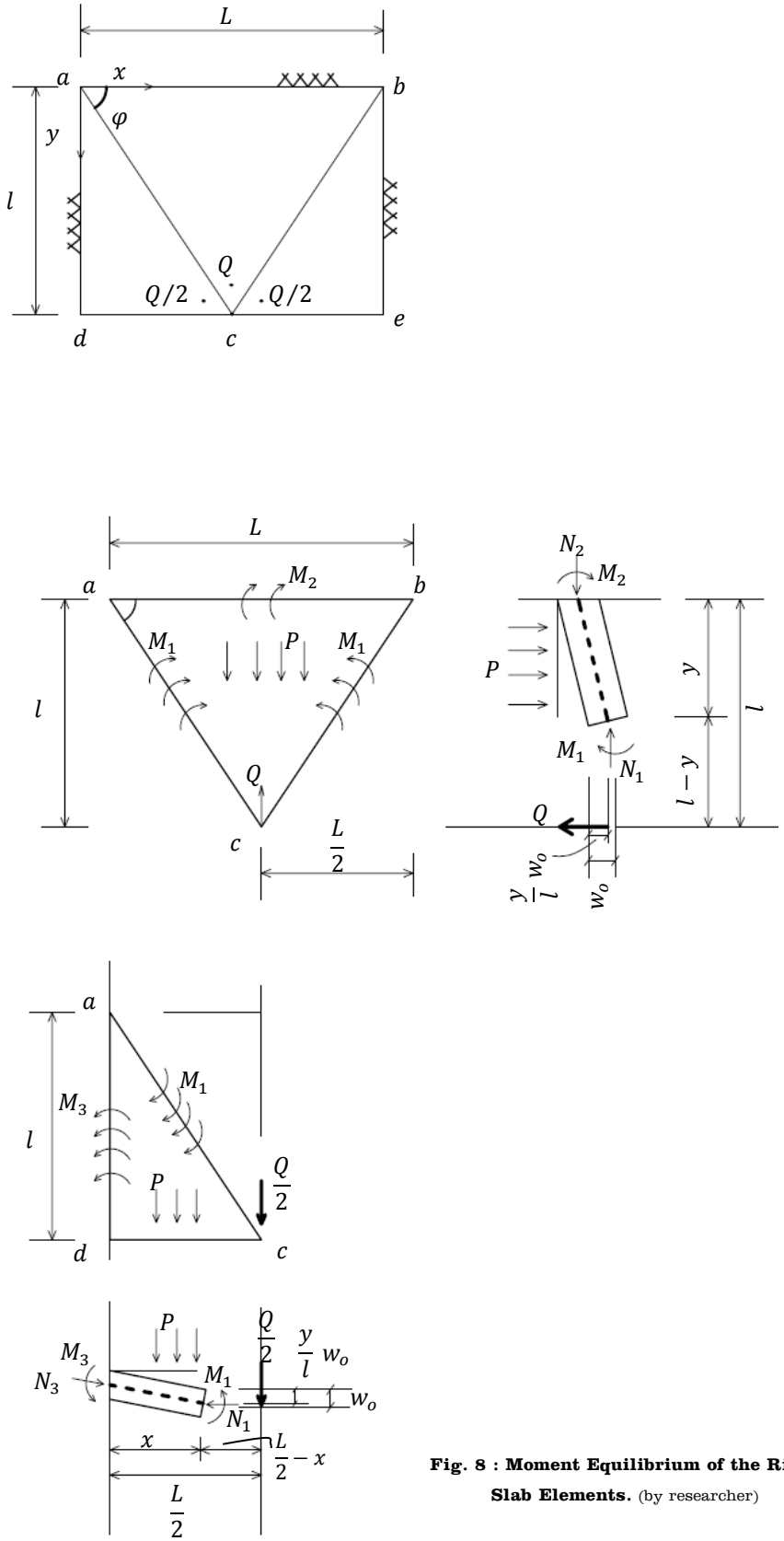

Fig. 8 : Moment Equilibrium of the Rigid Slab Elements. (by researcher)

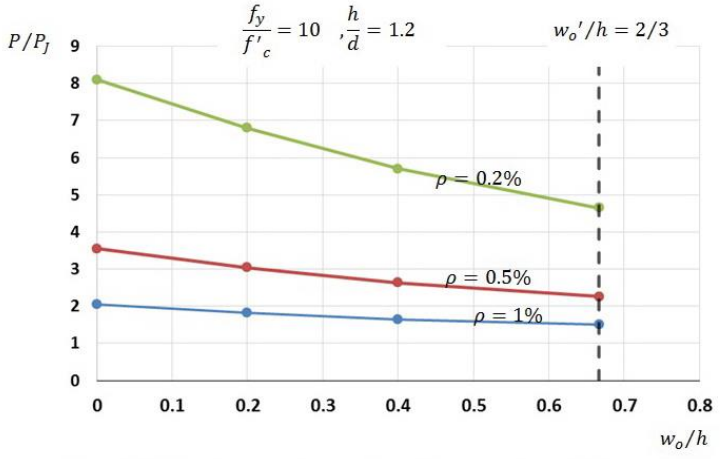

Fig. 9 : Effect of percentage of Reinforcement on P/P_J (by researcher)

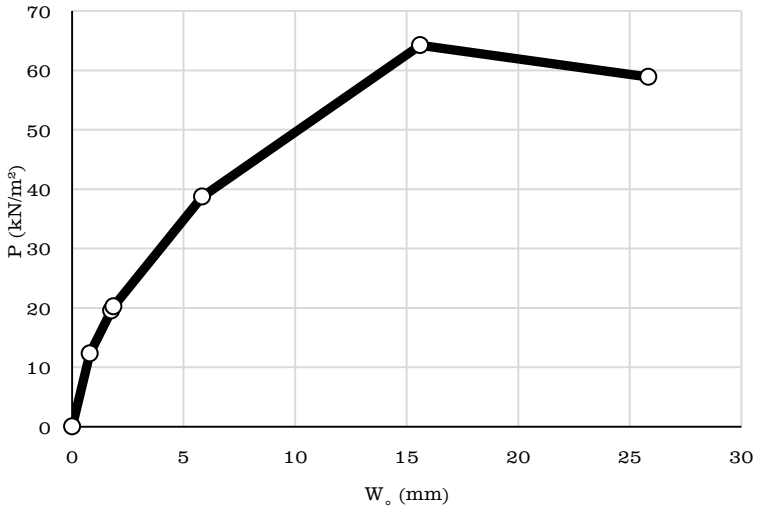

Fig. 10: Load-deflection curve. (by Researcher)